Influence of the Extrusion Process on the Morphology and Micromechanical Behavior of Polystyrene-*block*-(Polystyrene-*co*-Butadiene)-*block*-Polystyrene Star Block Copolymer/Homopolystyrene Blends

M. Buschnakowski,[1] R. Adhikari,[2] G. H. Michler,[1] K. Knoll[2]

[1]*Institute of Materials Science, University of Halle–Wittenberg, D-06099 Halle (Saale), Germany*
[2]*Polymer Research Thermoplastics, BASF Aktiengesellschaft, GKT/I-B1, D-67056 Ludwigshafen, Germany*

Received 9 February 2007; accepted 3 April 2007
DOI 10.1002/app.26753
Published online 20 July 2007 in Wiley InterScience (www.interscience.wiley.com).

ABSTRACT: The influence of the extrusion process on the morphology and micromechanical behavior of an asymmetric polystyrene-*block*-(polystyrene-*co*-butadiene)-*block*-polystyrene (SBS) star block copolymer and its blends with general-purpose homopolystyrene (hPS) was studied with films prepared with a single-screw extruder. The techniques used were transmission electron microscopy and uniaxial tensile testing. Unlike the pure SBS block copolymer possessing a gyroid-like morphology, whose deformation was found to be insensitive to the processing conditions, the mechanical properties of the blends strongly depended on the extrusion temperature as well as the apparent shear rate. The deformation micromechanism was primarily dictated by the blend morphology. The yielding and cavitation of the nanostructures were the principal deformation mechanism for the blends having a droplet-like microphase-separated morphology, whereas cavitation dominated for the blends containing macrophase-separated layers of polystyrene. The mechanical properties of the blends were further examined with respect to the influence of the temperature and shear rate on the phase behavior of the blends. © 2007 Wiley Periodicals, Inc. J Appl Polym Sci 106: 1939–1949, 2007

Key words: block copolymers; electron microscopy; extrusion; mechanical properties; phase behavior

INTRODUCTION

Research in the field of nanostructured materials, including block copolymers, has intensified in the last decade because of their promising optical, electrical, and mechanical properties. The wide spectrum of properties resulting from a variety of nanostructures is the reason behind the increasing interest in the study of many block copolymers of commercial significance.

The block copolymer phase behavior can be expressed by the product of χN, which is called the reduced interaction parameter;[1–3] χ and N stand for the Flory–Huggins segmental interaction parameter and the degree of polymerization, respectively. As a block copolymer cools from the melt, below a characteristic temperature called the order–disorder transition temperature, differently ordered nanostructures, popularly known as microphase-separated structures (e.g., body centered cubic spheres, hexagonal cylinders, gyroids, and lamellae), evolve. At sufficiently high molecular weights, the nature of the nanostructures to be formed at equilibrium is generally governed by the relative copolymer composition and the architectural constraints.[1–5] However, the influence of additional factors, such as the pressure and shear stress, that appear during the processing of commercial polymers (e.g., extrusion, injection, and compression molding) may cause a significant shift in the block copolymer phase behavior, leading to the evolution of morphologies not expected under equilibrium conditions. These changes arise not only from the reorganization of constituent block copolymer chains but also from the orientation of the nanostructures induced by shear stress. As demonstrated by various authors for different systems (e.g., body centered cubic spheres,[4,6,7] hexagonal cylinders,[8–14] and lamellae[15–17]), the shear-induced orientation behavior of the microphase-separated structures strongly depends on the temperature, shearing conditions, and molecular properties of the copolymer.

Correspondence to: G. H. Michler (goerg.michler@physik.uni-halle.de).

Contract grant sponsor: Kultusministerium des Landes Sachsen-Anhalt (to M.B. in the framework of the Stipendium zum 500-Jährigen Jubiläum der Martin-Luther Universität Halle–Wittenberg).

Contract grant sponsor: German Academic Exchange Service (to R. A. in support of his research stay at Martin-Luther Universität from September 2006 to October 2006 when the draft of this article was finalized).

Journal of Applied Polymer Science, Vol. 106, 1939–1949 (2007)

Because of their high production cost, styrene/diene block copolymers are generally mixed with homopolystyrene (hPS) to reduce the price. In such blends, the phase behavior is generally governed by the ratio of the degree of polymerization of the homopolymer to that of the corresponding block of the block copolymer. However, the phase-separation behavior (and hence the mechanical properties) of block copolymers[18,19] and their blends[20,21] are very sensitive to the processing conditions. Generally, the temperature and shear rate play opposite roles in the segregation behavior of blends showing upper critical solution temperature behavior. Stronger separation of contrary chains in blends occurs as the temperature decreases or the shear stress increases.[22–25]

Additionally, the orientation of the nanostructures induced by shear forces leads to a change in the mechanical properties. As shown by a series of micromechanical studies on different block copolymer systems (e.g., hexagonal cylinders,[26–30] gyroids,[31] and lamellae[20,21,32]), the orientation of the block copolymer nanostructures results in strongly anisotropic mechanical properties.

In the past, most studies have been devoted to understanding morphology formation in different styrenic block copolymers, their blends, and blends containing low-molecular-weight homopolymers [also with polystyrene (PS)]. However, for the commercial use of block copolymers, the morphologies formed at the thermodynamic equilibrium are less important, even though those studies have provided fundamental information about the phase behavior of block copolymer systems. Moreover, there has been a recent trend to develop PS-rich styrenic block copolymers possessing ductile behavior. The strategy is aimed at making the products more stable against degradation and more compatible with added PS. As a result, new block copolymer architectures have been introduced that have opened up new avenues in designing application-relevant block copolymer morphologies.

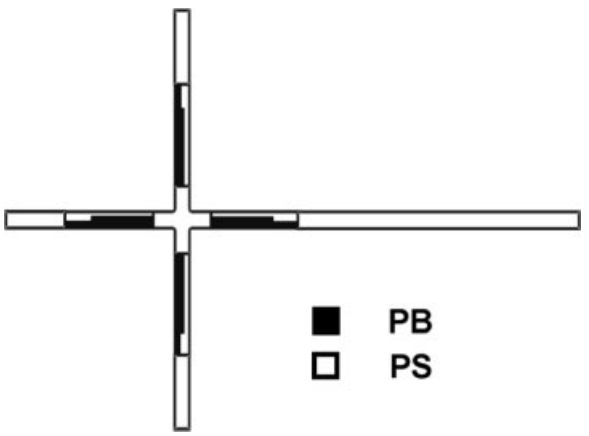

Figure 1 Scheme showing the chemical structure of the block copolymers. The bright and dark areas represent the PS and PB phases, respectively.

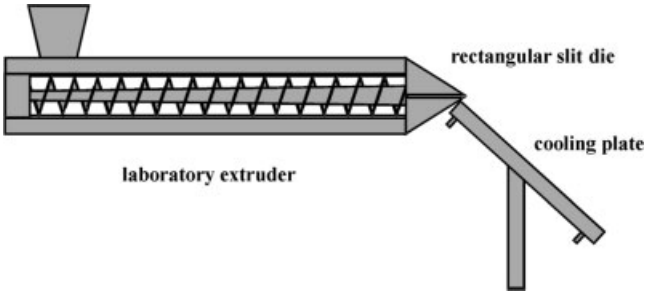

Figure 2 Schematic representation of the laboratory extruder with a rectangular slit die and cooling plate.

The goal of this work is to extend our previous studies on the blends of a new kind of styrene/butadiene star block copolymer and hPS[33] with oriented samples produced by means of a single-screw extruder. In particular, this article focuses on the development of the morphology under the influence of steady shear (during extrusion process) and its correlation with the deformation behavior of the blends.

EXPERIMENTAL

Materials

The block copolymer used in this work was a polystyrene-*block*-(polystyrene-*co*-butadiene)-*block*-polystyrene (SBS) star block copolymer (called ST3 here) having a number-average molecular weight (M_n) and polydispersity index [weight-average molecular weight/number-average molecular weight (M_w/M_n)] of 85,700 g/mol and 2.1, respectively. The molecular architecture of the star copolymer is shown schematically in Figure 1. The star-shaped molecules had approximately four arms, one of them much longer (molar mass = 61,000 g/mol) than the shorter ones (molar mass = 11,000 g/mol). The molecule had a PS core having a molecular weight of approximately 4500 g/mol.

Figure 1 shows that the copolymer was characterized by compositional and molecular asymmetry. The compositional asymmetry resulted from a total PS volume fraction of 0.74. Despite a high total PS content, the volume fraction of the soft phase was approximately 40%. The latter was a result of the presence of the polystyrene-*co*-polybutadiene (PS-*co*-PB) random copolymer middle block instead of pure polybutadiene (PB). The rubbery PS-*co*-PB middle block, which contained about 35% PS, was made up of two parts having different PS/PB ratios.

The hPS used, blended with ST3, was a commercial product (PS158k) of BASF. The M_w and M_w/M_n values of the hPS were 190,000 g/mol and 2.3,

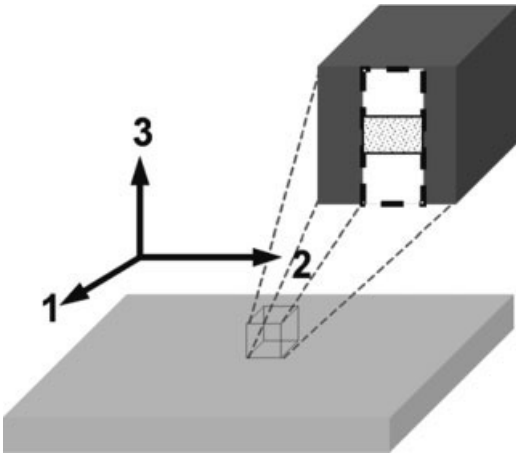

Figure 3 Scheme showing the preparation of a specimen from an extruded sheet for TEM examination: (1) transverse direction, (2) extrusion direction, and (3) shear gradient direction.

respectively. The investigated blends possessed 20, 40 and 60 wt % hPS. The blend compositions are expressed as weight fractions throughout the text.

Sample preparation

The sample films were prepared by extrusion with a single-screw extruder (Thermo-Haake, Karlsruhe, Germany; see the scheme in Fig. 2) at apparent shear rates of about 9, 312, and 683 s^{-1} with the variation of the extrusion temperature (180, 200, and 220°C). Before the melt blending, the components were mixed with a minidrum mixer (J. Engelsmann AG, Ludwigshafen, Germany). The extruder had a conventional three-zone screw (outside diameter = 19 mm) and a rectangular slit die (height = 0.5 mm, width = 100 mm; see Fig. 2). The strands coming out of the extruder were rapidly cooled to freeze the extrusion-process-induced phase-separated structures.

Tensile testing

The mechanical properties of selected films were determined parallel (direction 1 in Fig. 3) and perpendicularly to the extrusion direction (direction 2 in the Fig. 3) with a Zwick 1425 universal tensile machine (Zwick GmbH & Co., Ulm, Germany) at room temperature (23°C) and at a crosshead speed of 50 mm/min according to ISO 3167. The length and width of the resulting dog-bone-shaped tensile specimens were 50 and 4 mm, respectively.

Transmission electron microscopy (TEM)

The morphology of the samples was investigated with a transmission electron microscope (200 kV,

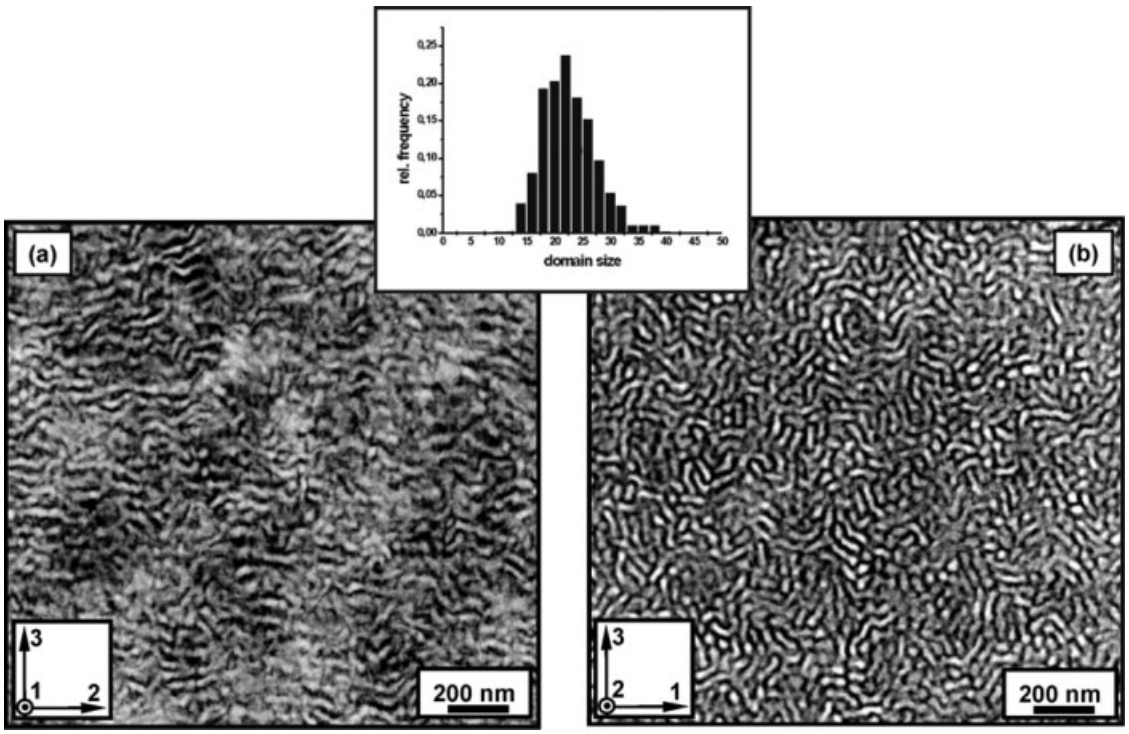

Figure 4 TEM micrographs showing the oriented gyroid-like structures and PS domain distributions in ST3 samples extruded at an apparent shear rate of ~9 s^{-1} and at 180°C. The TEM micrographs reflect the morphology in the middle of the films: (a) TEM along the transverse direction (direction 1) and (b) TEM along the extrusion direction (direction 2).

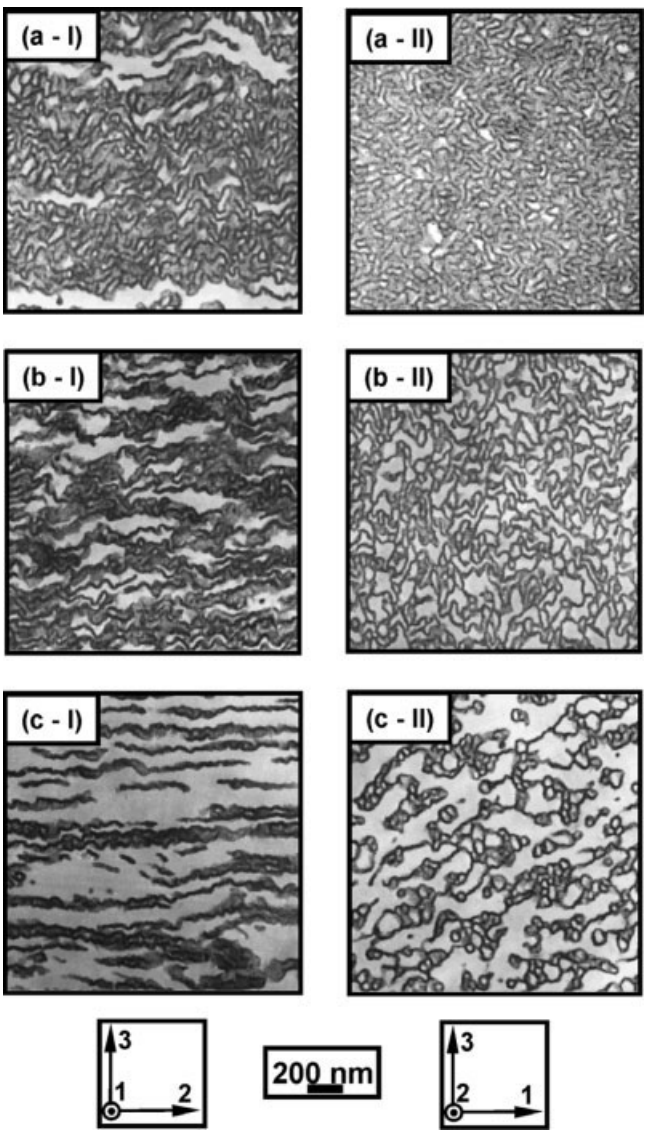

Figure 5 Morphology of ST3/hPS blends extruded at an apparent shear rate of 9 s^{-1} and at 200°C: (a) 20, (b) 40, and (c) 60% hPS. The left images show the morphology along the transverse direction, whereas the right ones show the morphology along the extrusion direction.

JEOL) along the whole cross section from two sides [the (1,3)-plane and (2,3)-plane of each film; see Fig. 3]. For these examinations, ultrathin sections (ca. 70 nm thick) were cut from a small block prepared from the respective bulk sample with the aid of a Leica Ultracut UCT ultramicrotome (Wetzlar, Germany) operated at room temperature. Before the sectioning, the specimens were treated with an aqueous osmium tetroxide (OsO_4) solution. Because of selective staining of the PB-rich phase by OsO_4, the PS-*co*-PB phase appeared darker in the TEM images, whereas the PS phase appeared bright. For the micromechanical investigations, the specimens were taken from deformed tensile bars from the locations close to the fracture surface.

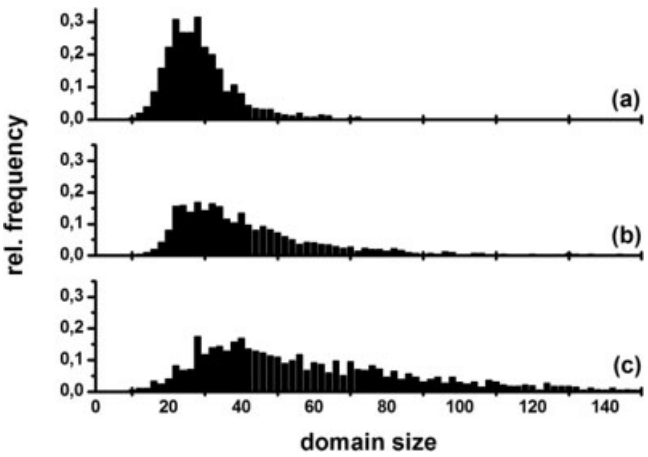

Figure 6 Domain size distributions of the droplet-like nanostructures with respect to the hPS content: (a) 20, (b) 40, and (c) 60% hPS.

RESULTS AND DISCUSSION

Morphology depending on the hPS content

In a diblock copolymer having comparable glassy-phase and rubbery-phase volume fractions (i.e., 60/40), such as ST3, a lamellar morphology would be expected. However, instead of the expected lamellar

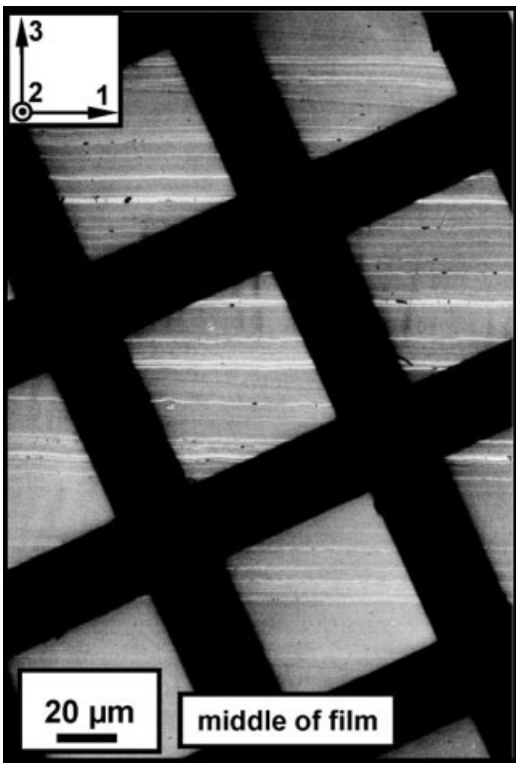

Figure 7 Low-resolution TEM images showing the formation of thick glassy layers through the cross section of an extruded blend (with 40% hPS). The film was extruded at an apparent shear rate of 312 s^{-1} and at 180°C; the black bars are from the grid.

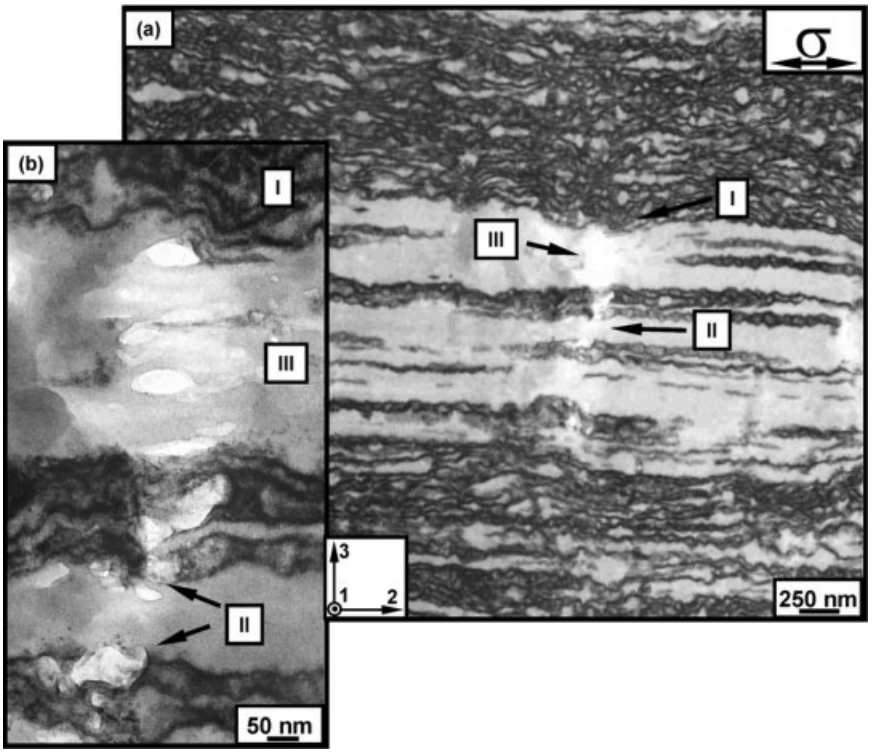

Figure 8 (a) Lower and (b) higher magnification TEM micrographs showing the morphology of an ST3/40% hPS blend after deformation (the extrusion conditions were the same as those for the blends in Fig. 5). Location I includes the yielding of droplet-like nanostructures, location II includes the cavitation of the droplet-like nanostructures and initiation of cavitation in the hard layers, and location III includes cavitation in the PS layers.

morphology, a gyroid-like morphology characterized by a continuous network of PS domains dispersed in the PS-*co*-PB rubbery matrix was observed that was independent of the processing methods. Figure 4 shows the morphology of the extruded star block copolymer along the (2,3)- and (1,3)-planes. The gyroid-like nanostructures were oriented in the extrusion direction (direction 2) under the influence of applied shear. The thickness of the PS domains was about 18 nm, and the interdomain spacing was approximately 32 nm. A detailed description of the morphology of ST3 with TEM has been reported in an earlier article.[35]

The TEM micrographs presented in Figure 5 show the morphological development in the extruded ST3/hPS blends as a function of the hPS content. The thickness distribution of the PS droplets measured in the TEM micrographs is collected in Figure 6. The TEM images show that the PS nanodomains were surrounded by an approximately 10-nm-thick continuous rubbery phase. The morphology of the blends comprised the PS phase in the form of irregular droplets of various sizes and hence could be termed a droplet-like nanostructure. This particular morphology was observed in corresponding compression-molded samples as well.[33,34] The droplet-like nanostructures, oriented along the extrusion direction, were found in all the extruded strands, regardless of the blend morphology (see Fig. 5).

The origin of the droplet-like morphology in the ST3/hPS blends might be correlated to the special architecture of the star block copolymer as well as the phase-separation behavior of the blend components. Actually, these structures were formed only in the blends that underwent macrophase separation at equilibrium. A decisive factor for the macrophase separation was a sufficiently large ratio of the molecular weight of the outer PS blocks of ST3 to that of hPS. The droplet-like PS domains, having variable sizes, resulted from the miscibility of different hPS chains with the outer PS blocks of ST3 having comparable molecular weights.

In the blends, the size of the nanostructures and their distribution shifted to higher values with the hPS content. Beyond 60% hPS, the droplet-like structures gradually disappeared, and the PS phase dominated the blend morphology [see Fig. 5(c)].

Besides the nanostructured droplets, macrophase-separated structures (e.g., glassy PS layers) were also formed in the blends. The details of the glassy layers are shown in Figure 7. These layers might have been formed by strongly separated hPS chains having molecular weights much larger than that of the largest outer PS block of ST3. The glassy layers, which were formed

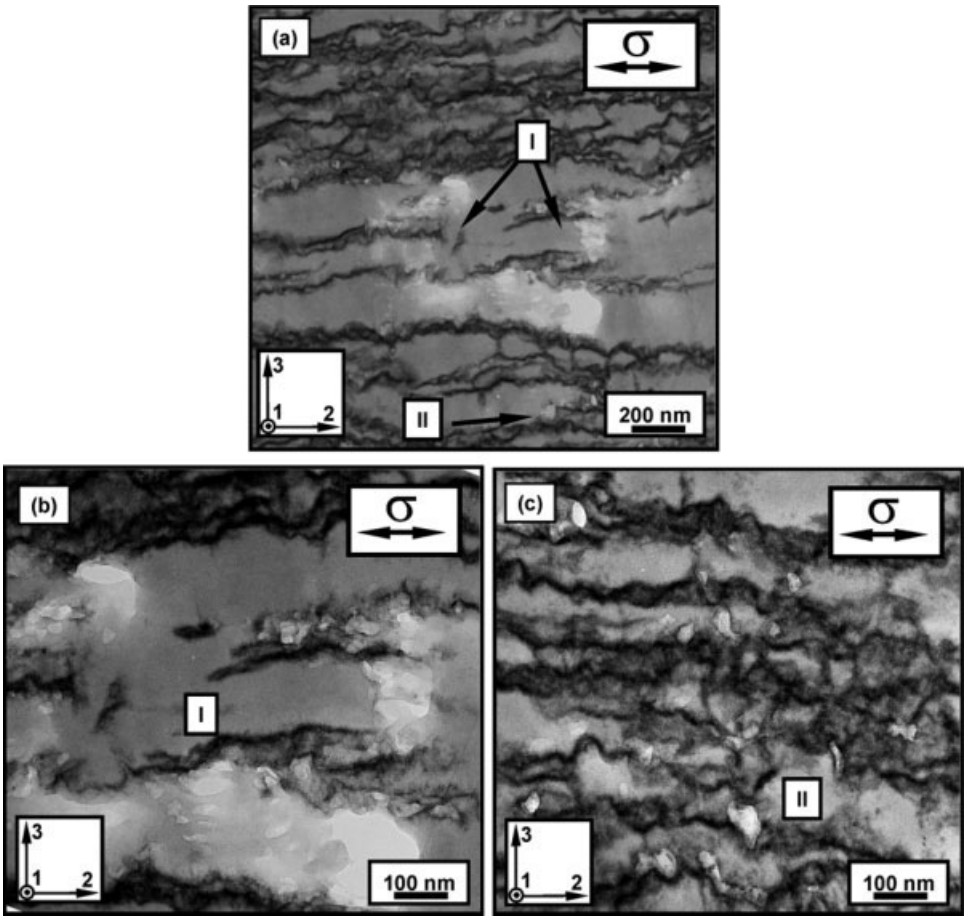

Figure 9 (a) Lower and (b,c) higher magnification TEM micrographs showing the morphology of an ST3/60% hPS blend after deformation (the extrusion conditions are the same as those for the blends in Fig. 5). Location I includes cavitation in the hard layers, and location II includes cavitation in the rubbery phase.

independently of the shear rate profile, were oriented in the extrusion direction. The increase in the hPS content led to the larger number of PS layers (see Fig. 7).

The morphology of the ST3/hPS blends, described in Figures 5–7, can be summarized as follows.

1. The morphology of the blends, dominated by the ST3 fraction, was characterized by both droplet-like nanostructures and macrophase-separated glassy layers.
2. With an increase in the hPS content, the number of PS layers increased, and that of the microphase-separated droplets decreased.
3. When hPS was the majority blend component, the effective droplet-like morphology collapsed, and the formation of the PS matrix began.

Deformation behavior of the ST3/hPS blends

The nanostructures of pure ST3, the smallest glassy domains of the system studied in this work, which were oriented along the extrusion direction, deformed plastically by a yielding and drawing mechanism. The deformation of the glassy PS domains was inhomogeneous, in the sense that regions with different levels of plastic deformation appeared along the glassy nanostructures. At large elongations, highly drawn struts of the glassy domains were formed. This observation was similar to the deformation behavior of block copolymers having oriented and unoriented gyroid morphology, as studied by Thomas and coworkers.[31,36] The glassy PS phase underwent irrecoverable plastic deformation on tensile loading.

During the deformation of extruded blends having a predominantly droplet-like morphology (e.g., blends with 20 or 40% hPS), two kinds of micromechanical processes appeared: cavitations of the glassy layers (e.g., Fig. 8, location III) and yielding of the microphase-separated droplet structures (e.g., Fig. 8, locations I and II).

The plastic deformation of the droplet-like nanostructures (i.e., yielding and drawing processes) was similar to the deformation of the gyroid-like morphology of ST3. Location I in Figure 8 shows that the PS droplets of the blend having 40% hPS deformed via yielding and drawing phenomena. The

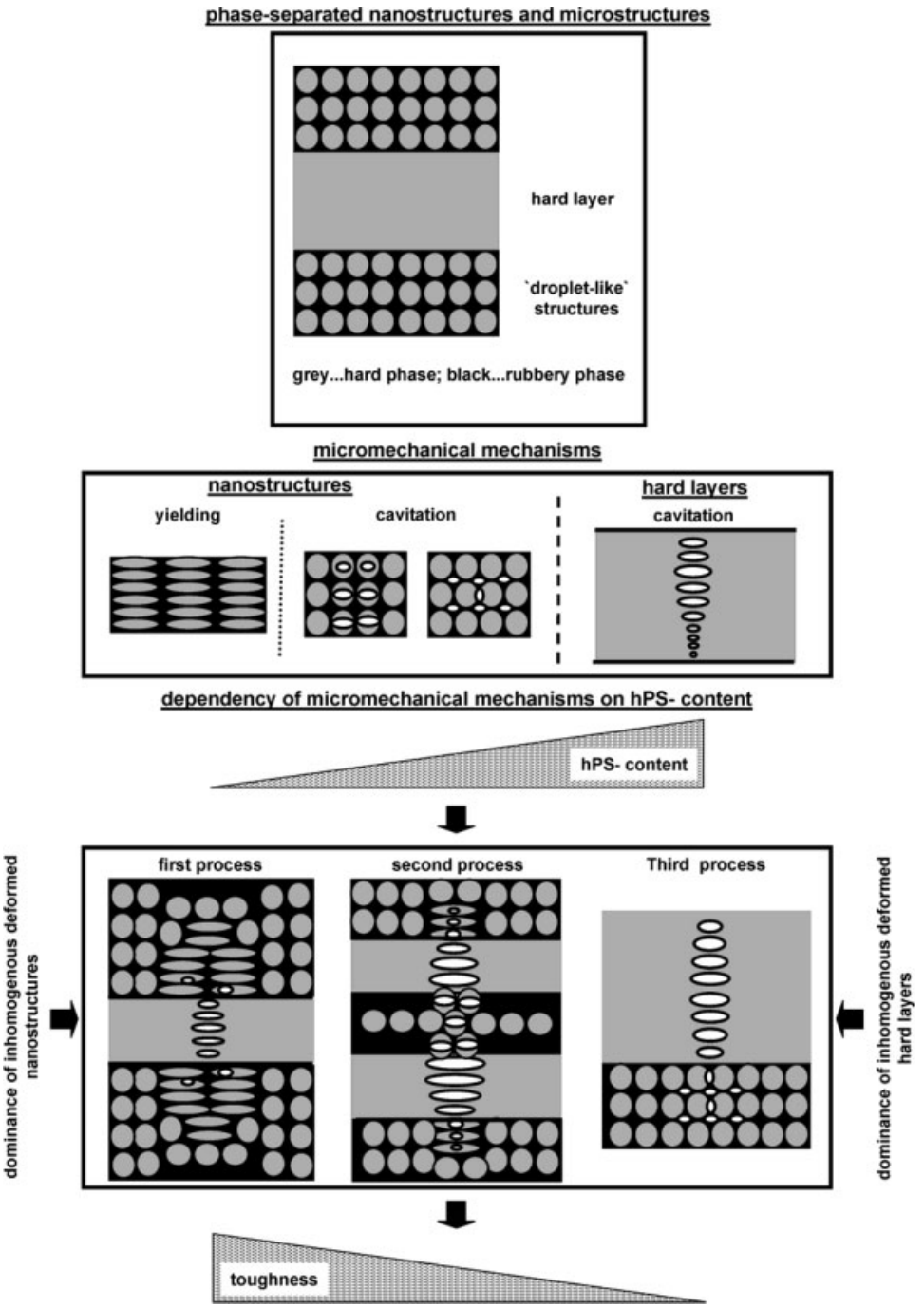

Figure 10 Scheme of the phase-separated structures and micromechanical mechanisms.

yielding of those hard inclusions (the droplets) was possible because of the stress transfer from the continuous rubbery phase to the hard inclusions.[37] This mechanism was analogous to the rubbery network toughening mechanisms observed in a poly(vinyl chloride)/ethylene vinyl acetate copolymer blend[38–40] and the mechanism of inclusion yielding or hard particle yielding observed in blends of polycarbonate and a polystyrene–acrylonitrile copolymer.[41,42] The nanostructures of the blends partly underwent very high deformation (up to ~ 4), as also proposed for fibrils in PS crazes.[43,44] The high plastic deformation of the droplet-like nanostructures in the blends was the reason for their high toughness. Besides the plastic yielding process discussed previously, cavitation of some of the microphase-separated glassy domains took place (location II in Fig. 8), and this actually affected the toughness of the blends in a negative way.

As mentioned earlier, the cavitation of glassy PS layers was another micromechanical process taking place during the uniaxial loading of the blends (see location III in Fig. 8). These cavitations could not

contribute to the toughness of the blends, but they led to decreasing toughness.

The blends containing hPS as the majority component (i.e., the blends with ≥60% hPS) had a morphology characterized by a PS matrix, whereas the droplet-like nanostructures were destroyed. Now the deformation of the blends took place mainly by cavitations (e.g., Fig. 9, location I) leading to a drastic reduction in the toughness. Additionally, microvoids were initiated in the soft phase of the blends (e.g., Fig. 9, location II), and this resembled the cavitation process observed previously in PS/PB diblock copolymers having PB cylinders embedded in a glassy PS matrix.[45,46]

Scheme of the micromechanical deformation processes

A summary of the micromechanical processes observed in the investigated blends is schematically illustrated in Figure 10. In particular, there was interplay between the drawing and cavitation mechanisms, depending on the overall morphology of the blends. The factors principally determining the kinds of deformation mechanisms and hence the toughness of the blends were the size and size distribution of the phase-separated structures. The observed mechanisms are summarized next.

Cavitation-stop mechanism

When the blend morphology was dominated by easily deformable nanostructured droplets (e.g., the blends with ≤40% hPS), the blends deformed via yielding; and no local deformation zones were formed. In this case, the stress in front of the local deformation zones was drastically reduced, with the result that the cavitation advancing through the PS layers was stopped because of plastic deformation of the surrounding matrix. This mechanism led to a large toughness value.

Cavitation

When the blends contained a large number of macrophase-separated glassy layers (and a reduced number of droplet-like nanostructures), the cavitation-stop mechanism would not work effectively. Then, the stress concentration in front of the local deformation zones located in a PS layer induced cavitation in the neighboring layers. As a result, the toughness of the blends decreased. At a high PS homopolymer content (≥60% hPS), the blends possessed the least toughness.

Mechanical behavior of the ST3/PS blends

The influence of the morphology and micromechanical processes discussed in the preceding sections was well reflected in the mechanical behavior of the blends. The dependence of the mechanical properties on the hPS content, as exemplified by the blends extruded at an apparent shear rate of about 9 s^{-1} and at 200°C, is illustrated by their tensile stress–strain curves given in Figure 11.

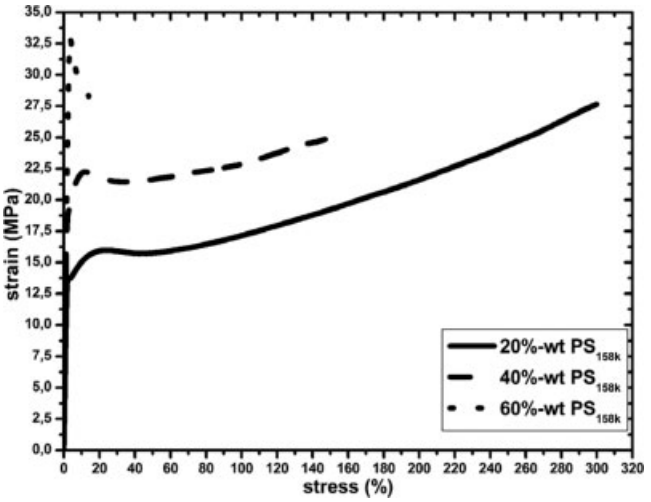

Figure 11 Stress–strain behavior of ST3/hPS blends (the morphology of the blends is presented in Fig. 5).

The star block copolymer showed a highly ductile behavior because of their molecular structure and resulting cocontinuous morphology.[35] As expected, the mechanical behavior of the blends continuously changed from tough behavior to brittle behavior with increasing hPS content. In the same order, the yield stress increased and the strain at break decreased. The strains at break of the blends with 20, 40, and 60% hPS were about 300, 150, and 12%, respectively. The ductile-to-brittle transition occurred at 60% PS when the droplet morphology began to disappear and the deformation mechanism was dominated by cavitation (which appeared macroscopically as stress whitening of the specimens during tensile testing).

The stress whitening was observed also for the blends containing 20 or 40% hPS and could be correlated with the combined effect of the yielding of droplet-like PS domains and cavitation in the glassy PS layers.

Effects of the extrusion temperature and apparent shear rate

Extrusion processes are determined by many factors, the most important ones being the temperature and shear rate. These are the decisive parameters for phase-separation behavior and morphology formation in block copolymers and blends with homopolymers. Consequently, the deformation behavior of these systems is also strongly affected. To demon-

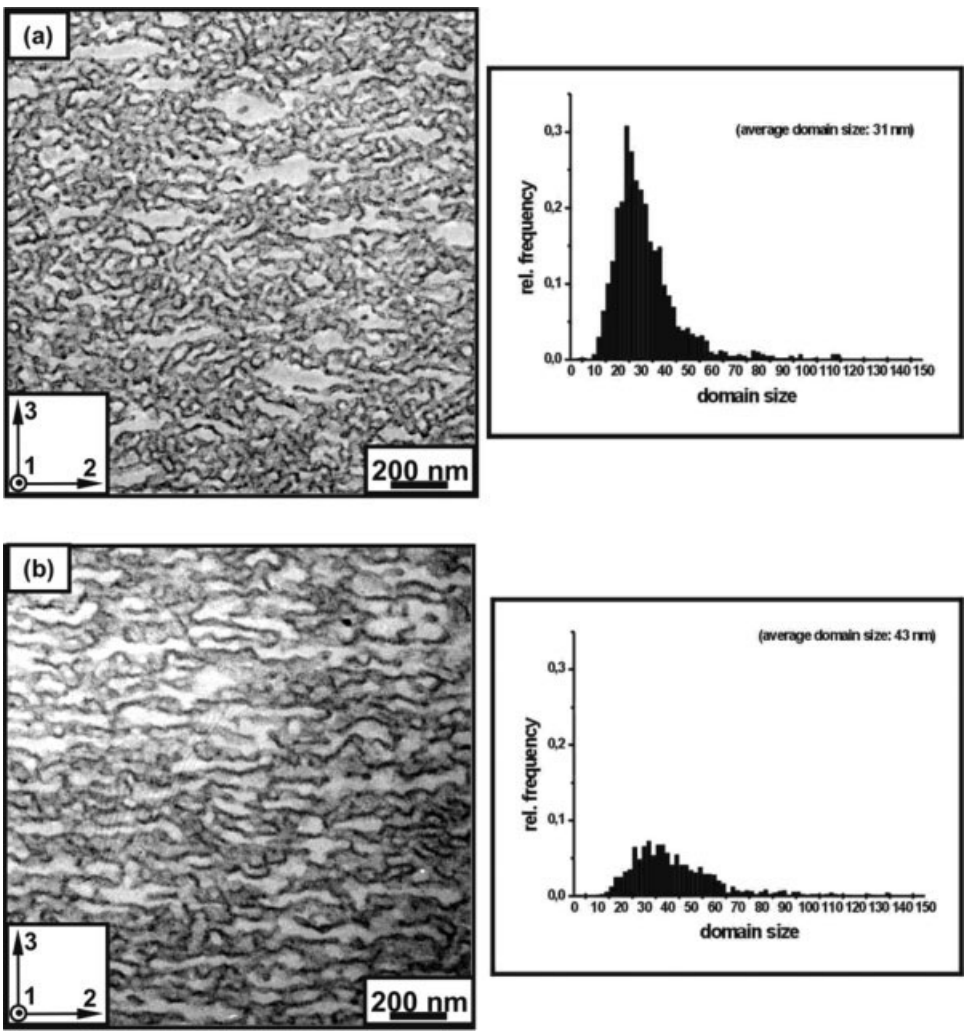

Figure 12 TEM micrographs and corresponding PS domain size distributions of an ST3/40% hPS blend extruded at an apparent shear rate of $\sim 312\ s^{-1}$ and at different temperatures: (a) 180 and (b) 220°C. The images reflect the morphology in the middle of the films.

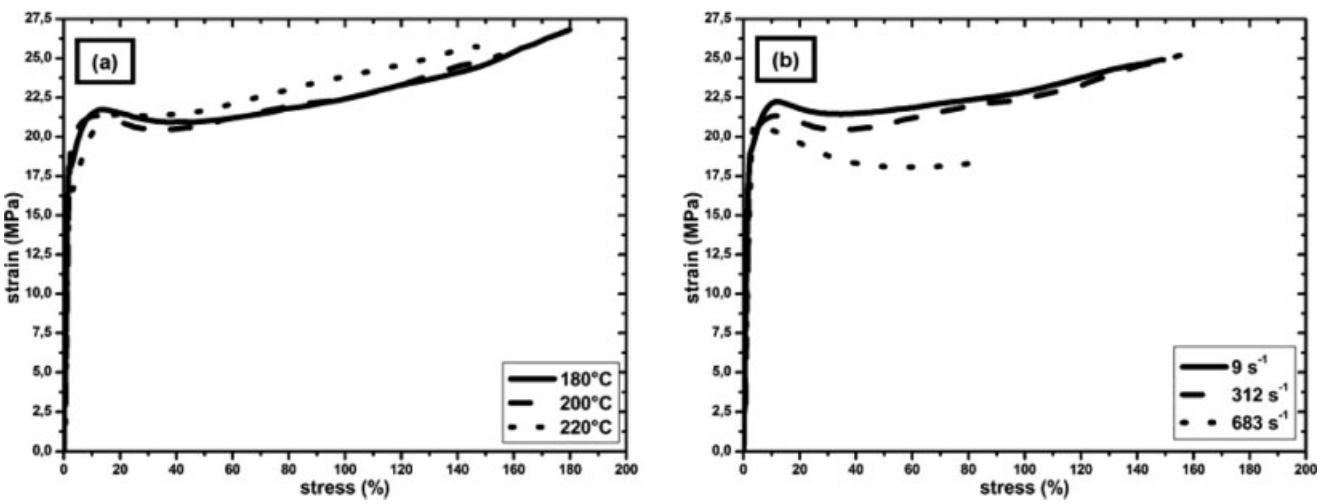

Figure 13 Dependence of the stress–strain behavior of a blend with 40% hPS on (a) the extrusion temperature and (b) the apparent shear rate.

strate the effect of these parameters on the morphology and mechanical properties, we briefly describe the results obtained for an ST3/40% hPS blend through changes in the extrusion temperature and shear rate. Figure 12 depicts TEM micrographs of the blend extruded at two different temperatures (180 and 220°C) with a constant shear rate of 312 s^{-1}. Similar structures were formed. The average domain sizes of the PS droplets in the blends extruded at 180 and 200°C were 30 and 43 nm, respectively. Moreover, the macrophase-separated layers of PS were not formed in the blends extruded at the higher temperature (220°C). This observation supports the assumption that the mixing effect dominated at the higher temperature rather than the lower one. An effect similar to that of the decreased extrusion temperature (e.g., the formation of PS layers) was observed with an increasing shear rate, which led to smaller microphase-separated droplets and a larger number of glassy layers.

Figure 13 shows tensile stress–strain diagrams of ST3/40% hPS blends prepared under different extrusion conditions. All the samples had identical compositions. In comparison with the temperature, the shear rate had a dramatic effect on the mechanical behavior of the blends. At a high shear rate, the toughness of the blends was drastically reduced, and this correlated well with the morphology of the blends formed (i.e., a larger number of PS layers formed).

CONCLUSIONS

Morphology formation in blends of a new kind of SBS block copolymer (ST3) and general-purpose hPS was studied. In particular, the effect of the morphology that formed on the mechanical behavior of the blends was analyzed. The results discussed in this article can be summarized as follows.

The studied star block copolymer formed a cocontinuous gyroid-like morphology, despite the high overall PS content. The morphology that formed was independent of the processing conditions. The deformation of the copolymer was characterized by highly ductile behavior.

Under the extrusion conditions, the ST3/hPS blends formed a special morphology comprising irregular droplets of PS embedded in a continuous rubbery matrix of the block copolymer. The observed structure has been termed a droplet-like morphology, and it was responsible for the observed high toughness of the blends.

Besides the droplet-like morphology, continuous layers of PS were also formed, whose number decreased as the extrusion temperature increased or the shear rate decreased. At a higher hPS concentration, the droplet-like morphology collapsed, and the extruded samples showed brittle behavior.

The droplet-like structures primarily deformed via a mechanism of microyielding followed by large plastic yielding, whereas the macrophase-separated layers deformed via cavitation. The toughness of the blends was determined by the interplay of these two mechanisms.

The authors thank Dr. K. Geiger and Mr. S. Danuningrat (Stuttgart, Germany) for providing the extruded sheets. Their sincere thanks go to the research groups of Profs. W. Grellmann and H.-J. Radusch for enabling the tensile testing and Ms. S. Goerlitz for the electron microscopy investigations. R. Adhikari kindly acknowledges the generous support from ZAV, Germany.

References

1. Balta Calleja, F. J.; Roslaniec, Z. Block Copolymers; Marcel Dekker: New York, 2000.
2. Thomas, E. L.; Lescanec, R. L. In Self-Order and Form in Polymeric Materials; Keller, A.; Warner, M.; Windle, A. H., Eds.; Chapman & Hall: London, 1995; Chapter 10.
3. Matshuhita, Y. In Structure and Properties of Multiphase Polymeric Materials; Araki, T.; Tankong, U.; Shibayama, M., Eds.; Marcel Dekker: New York, 1998; Chapter 5.
4. Hamley, I. W. The Physics of Block Copolymers; Oxford Science: Oxford, 1998.
5. Bates, F. S.; Fredrickson, G. H. AIP Phys Today 1999, 2, 32.
6. Koppi, K.; Bates, F. S. Macromolecules 1993, 26, 4058.
7. Koppi, K. A.; Tirrel, M.; Bates, F. S. J Rheol 1994, 38, 999.
8. Tepe, T.; Schulz, M. F.; Zhao, J.; Tirell, M.; Bates, F. S. Macromolecules 1995, 28, 3008.
9. Morrison, F. A.; Winter, H. H. Macromolecules 1989, 22, 3533.
10. Morrison, F. A.; Winter, H. H.; Gronski, W.; Barnes, J. D. Macromolecules 1990, 23, 4200.
11. Morrison, F. A.; Muthukumar, M.; Mays, J. W.; Nakatani, A. I.; Han, C. C. Macromolecules 1993, 26, 5271.
12. Jackson, C. L.; Barnes, K. A.; Morrison, F. A.; Mays, J. W.; Nakatani, A. I.; Han, C. C. Macromolecules 1995, 28, 713.
13. Folkes, M. J.; Keller, A.; Scalisi, F. P. Colloid Polym Sci 1973, 251, 1.
14. Keller, A.; Pedermonte, E.; Willmouth, F. M. Nature 1970, 225, 538.
15. Watanabe, H. In Structure and Properties of Multiphase Polymeric Materials; Araki, T.; Tran-Cong, Q.; Shibayama, M., Eds.; Marcel Dekker: New York, 1998; Chapter 9.
16. Chen, Z. R.; Issaian, M. A.; Kornfield, J. A.; Smith, D. S.; Grothaus, J. T.; Shatkowski, M. Macromolecules 1997, 30, 7096.
17. Chen, Z. R.; Kornfield, J. A. Polymer 1998, 39, 4679.
18. Weidisch, R.; Stamm, M.; Michler, G. H.; Fischer, H.; Jerome, R. Macromolecules 1999, 32, 742.
19. Weidisch, R.; Stamm, M.; Schubert, D. W.; Arnold, M.; Budde, H.; Höring, S. Macromolecules 1999, 32, 3405.
20. Michler, G. H.; Adhikari, R.; Lebek, W.; Goerlitz, S.; Weidisch, R.; Knoll, K. J Appl Polym Sci 2002, 85, 683.
21. Michler, G. H.; Adhikari, R.; Lebek, W.; Goerlitz, S.; Weidisch, R.; Knoll, K. J Appl Polym Sci 2002, 85, 701.
22. Almdal, K.; Mortensen, K.; Koppi, K. A.; Tirell, M.; Bates, F. S. J Phys II 1996, 6, 617.
23. Nakatani, A. I.; Morrison, F. A.; Douglas, J. F.; Mays, J. W.; Jackson, C. L.; Muthukumar, M.; Han, C. C. J Chem Phys 1996, 104, 1589.
24. Koppi, K. A.; Tirrel, M.; Bates, F. S. Macromolecules 1994, 27, 5934.

25. Cates, M. E.; Milner, S. T. Phys Rev Lett 1989, 62, 1856.
26. Villar, M. A.; Rueda, D. R.; Ania, F.; Thomas, E. L. Polymer 2000, 43, 5139.
27. Pakula, T.; Saijo, K.; Kawai, H.; Hashimoto, T. Macromolecules 1985, 18, 1294.
28. Honecker, C. C.; Thomas, E. L.; Albalak, R. J.; Hajduk, D. A.; Gruner, S. M.; Capel, M. C. Macromolecules 2000, 33, 9395.
29. Honecker, C. C.; Thomas, E. L. Macromolecules 2000, 33, 9407.
30. Sakurai, S.; Sakamoto, J.; Shibayma, M.; Nomura, S. Macromolecules 1993, 26, 3351.
31. Dair, B. J.; Avgeropoulos, A.; Hadjichristidis, N.; Thomas, E. L. J Mater Sci 2000, 35, 5207.
32. Cohen, Y.; Albalak, R. J.; Dair, B. J.; Capel, M. S.; Thomas, E. L. Macromolecules 2000, 33, 6502.
33. Buschnakowski, M.; Adhikari, R.; Ilisch, S.; Seydewitz, V. G. H.; Goderadt, R.; Lebek, W.; Michler, Knoll, K.; Schade, C. Macromol Symp 2006, 233, 66.
34. Buschnakowski, M. Ph.D. Thesis, University of Halle–Wittenberg, to be submitted.
35. Adhikari, R.; Buschnakowski, M.; Henning, S.; Goerlitz, S.; Huy, T. A.; Lebek, W.; Godehardt, R.; Michler, G. H.; Lach, R.; Geiger, K.; Knoll, K. Macromol Rapid Commun 2004, 25, 653.
36. Dair, B. J.; Honecker, C. C.; Alward, D. B.; Avgeropoulos, A.; Hadjichristidis, N.; Fetters, L. J.; Capel, M. S.; Thomas, E. L. Macromolecules 1999, 32, 8145.
37. Michler, G. H. In Mechanical Properties of Polymers Based on Nanostructure and Morphology; Michler, G. H.; Balta-Calleja, F. J., Eds.; Taylor & Francis: Boca Raton, FL, 2005; Chapter 10.
38. Michler, G. H.; Gruber, K. Plaste Kautsch 1976, 23, 346.
39. Michler, G. H. Polymer 1986, 27, 323.
40. Liu, Z. H.; Zhang, X. D.; Zhu, X. G.; Li, K. Y.; Wang, Z. N.; Choy, C. L. Polymer 1998, 39, 5035.
41. Kolarik, J.; Lednicky, F.; Locati, G.; Fambri, L. Polym Eng Sci 1997, 37, 128.
42. Kelnar, I.; Stephan, M.; Jakisch, L.; Fortelny, I. J Appl Polym Sci 1999, 74, 1404.
43. Michler, G. H. Kunststoff-Mikromechanik, Morphologie, Deformations- und Bruchmechanismen: Hanser: Munich, 1992.
44. Kramer, E. J. In Advances in Polymer Science; Kausch, H. H., Ed.; Springer-Verlag: Berlin, 1983; Vol. 52/53, p 1.
45. Koltisko, B.; Hiltner, A.; Bear, E. J. J Polym Sci Part B: Polym Phys 1986, 24, 2167.
46. Argon, A. S.; Cohen, R. E. In Advances in Polymer Science; Kausch, H. H., Ed.; Springer-Verlag: Berlin, 1983; Vol. 52/53.